

STRUCTURAL INVESTIGATION OF La/Mn CODOPED BISMUTH TITANATE CERAMIC PREPARED BY SOLID-STATE REACTION METHOD

M. S. Parvez¹ and M. Bodiul Islam^{2,*}

¹Department of Materials Science and Engineering (MSE), University of Rajshahi, Rajshahi-6205, Bangladesh

²Department of Glass and Ceramic Engineering (GCE), Rajshahi University of Engineering & Technology (RUET), Rajshahi-6204, Bangladesh

¹shaon_mst@yahoo.com, ^{2,*}mbislam_mst@yahoo.com

Abstract- Undoped bismuth titanate, $\text{Bi}_4\text{Ti}_3\text{O}_{12}$ (BIT), La doped bismuth titanate, $\text{Bi}_{3.25}\text{La}_{0.75}\text{Ti}_3\text{O}_{12}$ (BLT) and La/Mn codoped bismuth titanate $\text{Bi}_{3.25}\text{La}_{0.75}\text{Ti}_{3-x}\text{Mn}_x\text{O}_{12}$ (BLTM) ($x = 0.005, 0.01, 0.02$) ceramic samples were prepared by the solid state reaction method. The influence of La/Mn cosubstitution in the crystal structure was investigated by XRD and IR spectroscopy study. The XRD results show that all samples are polycrystalline and almost single phase with a bismuth-layered structure belonging to the crystalline phase BIT. Peak splitting of (hkl)/(khl) ($h \neq k$) peaks is observed in the XRD pattern of BIT and indicates that the crystal structure of BIT is monoclinic. Splitting of (hkl)/(khl) ($h \neq k$) peaks is reduced in BIT due to La doping that may related to the monoclinic to orthorhombic structural phase transition. The lattice parameter a decreases while b increases and the cell volume slightly decreases due to the doping. From IR spectra three absorption peaks are appeared at 814, 592 and 379 cm^{-1} , which is a characteristics feature of the formation of titanate structure. In addition two shoulder peaks are appeared at 313 and 470 cm^{-1} that could be related to the monoclinic symmetry of pure BIT. The absorption peaks at 592 and 379 cm^{-1} are shifted to higher wave number, while the intensity of the band at 814 cm^{-1} is significantly decreased and the shoulder peaks become disappear due to the addition of La that could be due to the monoclinic to orthorhombic structural phase transition. A new and relatively broad absorption peak is appeared around 1015 cm^{-1} due to Mn doping in BLT, which corresponds to the stretching vibration of Mn-O bonds. The intensity of 1015 cm^{-1} absorption peak gradually increases with the increase of Mn doping concentration indicates the substitution of Ti by Mn in the TiO_6 octahedron.

Keywords: Codoping, Solid-state reaction, XRD, IR

1. INTRODUCTION

Bismuth layered structure ferroelectrics (BLSFs) are one of the important class of ferroelectrics that have been synthesized by B. Aurivillius in 1949 [1, 2]. The chemical formula of this series is expressed $\text{Bi}_2\text{A}_{m-1}\text{B}_m\text{O}_{3m+3} = (\text{Bi}_2\text{O}_2)^{2+}(\text{A}_{m-1}\text{B}_m\text{O}_{3m+1})^{2-}$, where A can be mono-, di- or trivalent ions or a mixture of them, B represents tetra-, penta-, or hexavalent ions, and the subscripts m and $m-1$ ($m = 1, 2, \dots, 5$) are the numbers of oxygen octahedron and pseudo-perovskite units in the pseudo-perovskite layers, respectively. The crystal structure of BLSFs consists of pseudo-perovskite layers, which interleave bismuth oxide $(\text{Bi}_2\text{O}_2)^{2+}$ layers along the c -axis. A comprehensive research has been carried out since their invention due to a unique combination of properties, i.e. high Curie temperature (T_C), fatigue-free, and environmentally friendly nature, and have become potential candidates for electric and piezoelectric device applications.

Among BLSFs, ferroelectric $\text{Bi}_4\text{Ti}_3\text{O}_{12}$ (BIT) is a representative compound that has been extensively studied due to the unique combination of physical

properties and its lead-free chemical composition. The crystal structure of BIT is shown in Fig. 1. BIT crystal is water insoluble and has a density of 6.1 g/cm^3 . At room temperature, crystal structure of ferroelectric BIT is monoclinic phase with point group m , and it transforms into a paraelectric tetragonal phase with point group $4/mmm$ at T_{T-M} (675 °C) [3]. The bulk value of the remanent polarization ($2P_r$) of BIT is about 98 $\mu\text{C}/\text{cm}^2$; however, in its thin films, it decreases unexpectedly down to low values of 4 - 8 $\mu\text{C}/\text{cm}^2$ because of repeated polarization switching. BIT is considered to be a potential candidate for lead-free chemical composition, high $2P_r$, and other good electrical properties. However, it suffers from a strong fatigue failure after 10^{12} cycles and high processing temperature. Recently, it has been reported that A-site modification in BIT by using Lanthanides (La, Pr, Sm and Nd) improves fatigue behavior significantly. Among them, the La doped BIT, namely $\text{Bi}_{3.25}\text{La}_{0.75}\text{Ti}_3\text{O}_{12}$, ceramics shows completely fatigue free under repeating switching cycle but in this case the $2P_r$ decreases largely from 50 $\mu\text{C}/\text{cm}^2$ to 30 $\mu\text{C}/\text{cm}^2$ while the $2E_c$, 100KV cm^{-1} , is reasonable.

Many researcher reported that B-site modification in BIT enhance the $2Pr$ with containing the fatigue free behavior. Therefore, B-site modification is necessary to improve the $2Pr$. In the present investigation, Mn ion is chosen for the B-site modification of La doped BIT because Mn ion shows a peculiar behavior due to variable valences such as Mn^{2+} , Mn^{3+} , Mn^{4+} .

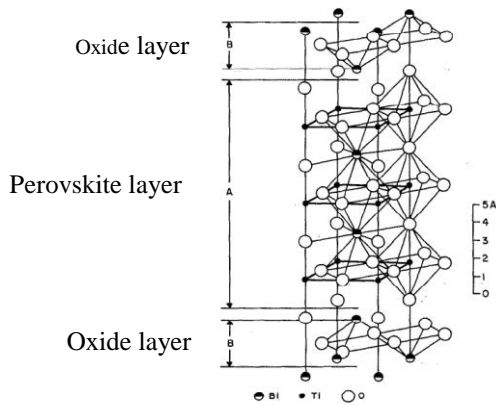


Fig.1: Crystal structure of $Bi_4Ti_3O_{12}$ [2]

2. EXPERIMENTAL PROCEDURE

Pure BIT, La-doped BIT and La/Mn codoped BIT samples were prepared by the solid-state reaction method. A reagent grade Bi_2O_3 (MERCK, Germany), La_2O_3 (Wako Pure Chemical Industries Ltd., Japan), TiO_2 (MERCK Ltd., Mumbai, India) and MnO_2 (Wako Pure Chemical Industries Ltd., Japan) powders have been used as the starting materials. Sample preparation has been completed by the following steps:

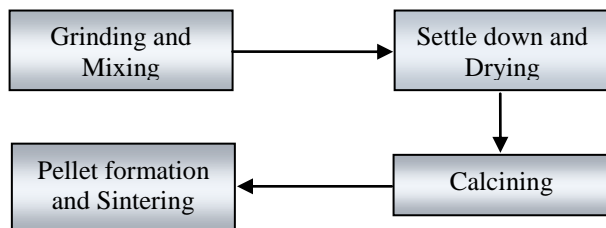


Fig.2. Different steps of sample preparation

First stoichiometric amounts of starting materials were weighted out and then the weighted powders were milled in ethanol for 24 hours in a ball mill. After ball milling the mixture was kept in a beaker for 24 hours to precipitate the mixed powder at the bottom of the beaker. The ethanol was removed from the upper portion and the precipitate powders were put into an oven for drying. The dried powder was then grounded in a mortar pestle to form fine powder and calcined at $800\text{ }^\circ\text{C}$ for 4 hours. The rate of temperature raising and cooling was maintained at $10\text{ }^\circ\text{C}$ per minute. The calcined powders mixed with 2.5% PVA solution in a mortar pestle and then pressed at 60 KN to form pellet. The prepared pellets were then sintered at $1050\text{ }^\circ\text{C}$ for 1 hour. The color of $Bi_4Ti_3O_{12}$ and $Bi_{3.25}La_{0.75}Ti_3O_{12}$ is white shadow, $Bi_{3.25}La_{0.75}Ti_{2.995}Mn_{0.005}O_{12}$ is brown shadow, $Bi_{3.25}La_{0.75}Ti_{2.99}Mn_{0.01}O_{12}$ is light brown and $Bi_{3.25}La_{0.75}Ti_{2.98}Mn_{0.02}O_{12}$ is brown.

Here we used natural convection oven (JSR, JSON-100) for drying. Carbolite furnace (ELF 11/6B) was used for calcining and sintering. Shimadzu hand pressure gauge machine was used for the formation of pellet. X-ray diffraction pattern of the powder samples were taken by using an X-ray diffractometer (X'Pert-PRO, Philips, Japan) to study the phase formation and purity of the prepared samples. All infrared spectra of the samples were collected by FTIR spectrophotometer (spectrum 100, Perkin Elmer) over the range of wave number $2000 - 300\text{ cm}^{-1}$. The resolution of the instrument was 1 cm^{-1} . For the measurement of dielectric constant of the prepared samples we have used Precision Impedance Analyzer (Model 4294A, Agilent Technologies, Japan.).

3. RESULTS AND DISCUSSION

The experimental results and possible explanations of various measurements of pure $Bi_4Ti_3O_{12}$ (BIT), La doped BIT, $Bi_{3.25}La_{0.75}Ti_3O_{12}$ (BLT) and, La and Mn doped BIT, $Bi_{3.25}La_{0.75}Ti_{2.98}Mn_{0.02}O_{12}$ (BLTM) samples have been given in this section.

3.1 Study of XRD

The structure and phase of the sintered BIT, BLT and BLTM samples were characterized by X-ray diffraction (XRD) using $Cu\ K\alpha$ ($\lambda = 1.5405\text{ \AA}$) radiation. The scanning drive axis is taken as two-theta and the scan was recorded in between 10 to 60 degree of 2θ values for some of the selected compositions. The values of miller indices (hkl) were identified from reference code 36-1486. The lattice parameters of the samples were determined by using the equation

$$1/(d_{hkl})^2 = h^2/a^2 + k^2/b^2 + l^2/c^2 \quad (1)$$

where, d_{hkl} is the inter planer spacing and h, k and l is miller indices.

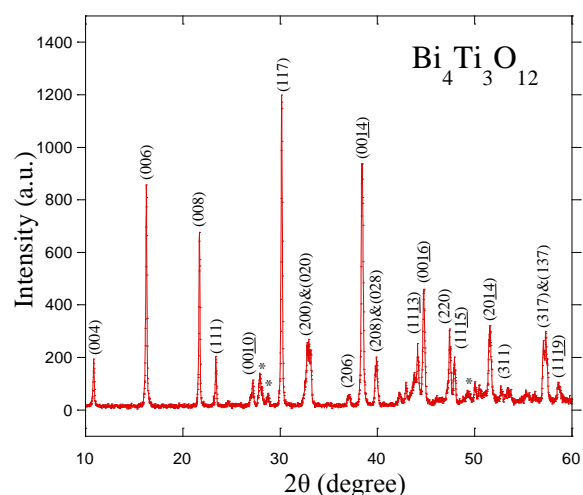


Fig.3: X-ray diffraction patterns of BIT ceramic sample sintered at $1050\text{ }^\circ\text{C}$ for 1 hour. (*Pyrochlore phase)

The X-ray diffraction patterns of BIT ceramic sample sintered at $1050\text{ }^\circ\text{C}$ for 1 hour is shown in Fig. 3. All the peaks are indexed according to the reference code 36-1486, which indicates that the obtained BIT ceramic is polycrystalline in nature and almost single phase of

bismuth-layered perovskite structure with preferred (117) and (00l) orientations [4]. In the XRD pattern of BIT, peak splitting of (hkl)/(khl) ($h \neq k$) peaks is observed. This can be explained as follows. Meta-stable tetragonal BIT was formed in the prepared BIT sample at low temperature. When the synthesis temperature was sufficiently high, monoclinic or pseudo-orthorhombic BIT was formed and the difference in the lattice parameters between a and b ($a = 0.54641$ nm, $b = 0.54088$ nm) led to the splitting of the (hkl)/(khl) peaks [5]. However, in the XRD pattern there are three unknown peaks observed at (27.9198°), (28.7277°) and (49.3098°) respectively. These collective peaks indicate that a trace amount of another phase is present in the sample. This phase could be pyrochlore ($\text{Bi}_2\text{Ti}_2\text{O}_7$) phase [6]. The peak position, corresponding Miller indices and possible phase of the sample is tabulated in Table 1. In addition, the slim width of the diffraction peaks indicates the large grain size of the ceramic [7].

Table 1: The peak position, corresponding Miller indices and possible phase of the sample of $\text{Bi}_4\text{Ti}_3\text{O}_{12}$

No. of peak	Peak position ($^\circ 2\theta$)	d-spacing (\AA)	Relative Int. (%)	Miller indices (h k l)	Possible Phase
1	10.84	8.15	15.34	0 0 4	$\text{Bi}_4\text{Ti}_3\text{O}_{12}$
2	16.26	5.44	71.09	0 0 6	$\text{Bi}_4\text{Ti}_3\text{O}_{12}$
3	21.70	4.09	55.94	0 0 8	$\text{Bi}_4\text{Ti}_3\text{O}_{12}$
4	23.39	3.80	15.83	1 1 1	$\text{Bi}_4\text{Ti}_3\text{O}_{12}$
5	27.19	3.27	7.68	0 0 10	$\text{Bi}_4\text{Ti}_3\text{O}_{12}$
6	27.91	3.19	8.94	---	$\text{Bi}_2\text{Ti}_2\text{O}_7$
7	28.72	3.10	2.92	---	$\text{Bi}_2\text{Ti}_2\text{O}_7$
8	30.14	2.96	100	1 1 7	$\text{Bi}_4\text{Ti}_3\text{O}_{12}$
9	32.78	2.73	19.71	2 0 0	$\text{Bi}_4\text{Ti}_3\text{O}_{12}$
10	33.19	2.69	14.77	0 2 0	$\text{Bi}_4\text{Ti}_3\text{O}_{12}$
11	37.04	2.42	2.62	2 0 6	$\text{Bi}_4\text{Ti}_3\text{O}_{12}$
12	38.41	2.34	76.70	0 0 14	$\text{Bi}_4\text{Ti}_3\text{O}_{12}$
13	39.78	2.26	11.40	2 0 8	$\text{Bi}_4\text{Ti}_3\text{O}_{12}$
14	39.92	2.25	13.77	0 2 8	$\text{Bi}_4\text{Ti}_3\text{O}_{12}$
15	44.16	2.04	15.97	1 1 13	$\text{Bi}_4\text{Ti}_3\text{O}_{12}$
16	44.75	2.02	36.34	0 0 16	$\text{Bi}_4\text{Ti}_3\text{O}_{12}$
17	47.41	1.91	23.68	2 2 0	$\text{Bi}_4\text{Ti}_3\text{O}_{12}$
18	47.90	1.89	12.57	1 1 15	$\text{Bi}_4\text{Ti}_3\text{O}_{12}$
19	49.30	1.84	2.64	---	$\text{Bi}_2\text{Ti}_2\text{O}_7$
20	51.57	1.77	22.37	2 0 14	$\text{Bi}_4\text{Ti}_3\text{O}_{12}$
21	53.46	1.71	3.10	3 1 1	$\text{Bi}_4\text{Ti}_3\text{O}_{12}$
22	57.06	1.61	16.15	3 1 7	$\text{Bi}_4\text{Ti}_3\text{O}_{12}$
23	57.29	1.60	22.08	1 3 7	$\text{Bi}_4\text{Ti}_3\text{O}_{12}$
24	58.59	1.57	5.52	1 1 19	$\text{Bi}_4\text{Ti}_3\text{O}_{12}$

Fig. 4 shows the X-ray diffraction patterns of the BLT ceramic sample sintered at 1050°C for 1 hour. The XRD peaks of the BLT ceramics are similar to that of BIT ceramics. The layered perovskite (117) and (00l) peaks were found in XRD patterns, which agreed with peaks of BIT ceramics. This indicates that BLT single phases having Bi-layer structured ferroelectrics crystal structure were confirmed for the La content [8]. No peak splitting is observed in the XRD pattern of BLT sample. This can be explained as follows. The BIT ceramic undergoes a structural phase transition from monoclinic or

pseudo-orthorhombic to orthorhombic phases due to La doping. Because of the very similar lattice parameters a and b ($a = 0.54236$ nm, $b = 0.54132$ nm) of orthorhombic BLT, no splitting of the (hkl)/(khl) peaks could be detected [6].

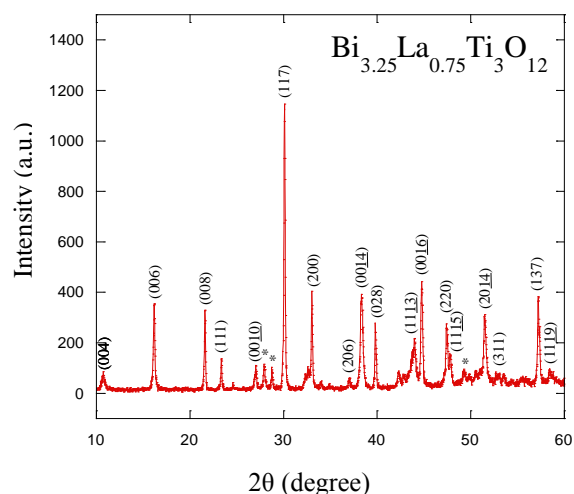


Fig.4: X-ray diffraction patterns of BLT ceramic sample sintered at 1050°C for 1 hour. *Pyrochlore phase

The relative intensity of (00l) to (117) peaks decrease as the La is doped in BIT. This indicates that a small change in crystallographic orientation occur due to La doping in BIT. There are also three unknown peaks are observed in the XRD pattern of BLT, this indicates that small amount of pyrochlore ($\text{Bi}_2\text{Ti}_2\text{O}_7$) phase are also present in the BLT ceramic. The peak position, corresponding Miller indices and possible phase of the sample is tabulated in Table 2.

Table 2: The peak position, corresponding Miller indices and possible phase of the sample of $\text{Bi}_{3.25}\text{La}_{0.75}\text{Ti}_3\text{O}_{12}$

No. of peak	Peak position ($^\circ 2\theta$)	d-spacing (\AA)	Relative Int. (%)	Miller indices (h k l)	Possible Phase
1	10.71	8.25	5.74	0 0 4	$\text{Bi}_4\text{Ti}_3\text{O}_{12}$
2	16.19	5.47	30.09	0 0 6	$\text{Bi}_4\text{Ti}_3\text{O}_{12}$
3	21.60	4.11	28.23	0 0 8	$\text{Bi}_4\text{Ti}_3\text{O}_{12}$
4	23.35	3.80	10.35	1 1 1	$\text{Bi}_4\text{Ti}_3\text{O}_{12}$
5	27.04	3.29	7.23	0 0 10	$\text{Bi}_4\text{Ti}_3\text{O}_{12}$
6	27.93	3.19	7.82	---	$\text{Bi}_2\text{Ti}_2\text{O}_7$
7	28.76	3.10	6.73	---	$\text{Bi}_2\text{Ti}_2\text{O}_7$
8	30.09	2.96	100	1 1 7	$\text{Bi}_4\text{Ti}_3\text{O}_{12}$
9	33.03	2.71	34.08	2 0 0	$\text{Bi}_4\text{Ti}_3\text{O}_{12}$
10	37.01	2.42	3.56	2 0 6	$\text{Bi}_4\text{Ti}_3\text{O}_{12}$
11	38.33	2.34	31.45	0 0 14	$\text{Bi}_4\text{Ti}_3\text{O}_{12}$
12	39.81	2.26	22.43	0 2 8	$\text{Bi}_4\text{Ti}_3\text{O}_{12}$
13	44.00	2.05	16.68	1 1 13	$\text{Bi}_4\text{Ti}_3\text{O}_{12}$
14	44.75	2.02	34.00	0 0 16	$\text{Bi}_4\text{Ti}_3\text{O}_{12}$
15	47.40	1.91	21.76	2 2 0	$\text{Bi}_4\text{Ti}_3\text{O}_{12}$
16	47.79	1.90	10.77	1 1 15	$\text{Bi}_4\text{Ti}_3\text{O}_{12}$
17	49.26	1.84	4.94	---	$\text{Bi}_2\text{Ti}_2\text{O}_7$
18	51.49	1.77	23.22	2 0 14	$\text{Bi}_4\text{Ti}_3\text{O}_{12}$
19	53.53	1.71	3.14	3 1 1	$\text{Bi}_4\text{Ti}_3\text{O}_{12}$
20	57.20	1.60	30.12	1 3 7	$\text{Bi}_4\text{Ti}_3\text{O}_{12}$
21	58.46	1.57	3.92	1 1 19	$\text{Bi}_4\text{Ti}_3\text{O}_{12}$

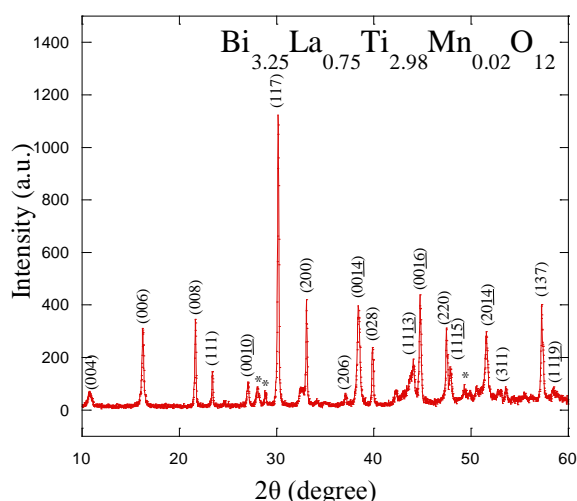


Fig.5: X-ray diffraction patterns of BLTM ceramic sample sintered at 1050 °C for 1 hour. *Pyrochlore phase

Fig. 5 shows the XRD patterns of the BLTM ceramic with Mn content ($x=0.02$). The XRD peaks of the BLTM ceramic are similar to that of BIT ceramic. The layered perovskite (117) and (00 l) peaks were found in XRD patterns, which agreed with peaks of BIT ceramics. This confirms that the obtained BLTM ceramic was polycrystalline and almost single phase of bismuth-layered perovskite structure [4]. The position of diffraction peaks of the BLTM ceramic is in agreement with that of standard diffraction peaks of BIT, indicating Mn substitution does not change the layered structure [4].

Table 3: The peak position, corresponding Miller indices and possible phase of the sample of $\text{Bi}_{3.25}\text{La}_{0.75}\text{Ti}_{2.98}\text{Mn}_{0.02}\text{O}_{12}$

No. of peak	peak position (°2θ)	d-spacing (Å)	Relative Int. (%)	Miller indices (h k l)	Possible Phase
1	10.76	8.21	4.89	0 0 4	$\text{Bi}_4\text{Ti}_3\text{O}_{12}$
2	16.25	5.45	24.91	0 0 6	$\text{Bi}_4\text{Ti}_3\text{O}_{12}$
3	21.65	4.10	30.08	0 0 8	$\text{Bi}_4\text{Ti}_3\text{O}_{12}$
4	23.39	3.80	12.06	1 1 1	$\text{Bi}_4\text{Ti}_3\text{O}_{12}$
5	27.06	3.29	7.24	0 0 10	$\text{Bi}_4\text{Ti}_3\text{O}_{12}$
6	28.04	3.18	6.19	- - -	$\text{Bi}_2\text{Ti}_2\text{O}_7$
7	28.87	3.09	4.21	- - -	$\text{Bi}_2\text{Ti}_2\text{O}_7$
8	30.15	2.96	100	1 1 7	$\text{Bi}_4\text{Ti}_3\text{O}_{12}$
9	33.08	2.70	36.57	2 0 0	$\text{Bi}_4\text{Ti}_3\text{O}_{12}$
10	37.08	2.42	3.52	2 0 6	$\text{Bi}_4\text{Ti}_3\text{O}_{12}$
11	38.41	2.34	34.22	0 0 14	$\text{Bi}_4\text{Ti}_3\text{O}_{12}$
12	39.85	2.26	19.29	0 2 8	$\text{Bi}_4\text{Ti}_3\text{O}_{12}$
13	44.08	2.05	13.49	1 1 13	$\text{Bi}_4\text{Ti}_3\text{O}_{12}$
14	44.75	2.02	37.05	0 0 16	$\text{Bi}_4\text{Ti}_3\text{O}_{12}$
15	47.45	1.91	25.73	2 2 0	$\text{Bi}_4\text{Ti}_3\text{O}_{12}$
16	47.87	1.90	10.85	1 1 15	$\text{Bi}_4\text{Ti}_3\text{O}_{12}$
17	49.31	1.84	3.94	- - -	$\text{Bi}_2\text{Ti}_2\text{O}_7$
18	51.58	1.77	22.86	2 0 14	$\text{Bi}_4\text{Ti}_3\text{O}_{12}$
19	53.58	1.71	3.82	3 1 1	$\text{Bi}_4\text{Ti}_3\text{O}_{12}$
20	57.24	1.60	32.80	1 3 7	$\text{Bi}_4\text{Ti}_3\text{O}_{12}$
21	58.56	1.57	2.78	1 1 19	$\text{Bi}_4\text{Ti}_3\text{O}_{12}$

Moreover, there is no obvious difference in the XRD patterns of the BLTM ceramic from XRD patterns of the BLT ceramic which indicates that there is no influence in the crystal orientation due to the Mn substitution [4]. The peaks position, corresponding Miller indices and possible phase of the samples are tabulated in Table 3. The lattice parameters a , b , c and cell volume of BIT, BLT and BLTM ceramic sample are calculated using (200), (028) and (008) planes and tabulated in Table 4. From table it is found that the lattice parameters a decrease and b increase with La and Mn doping. The cell volume slightly decreases with the doping.

Table 4: Lattice constant ' a ', ' b ', ' c ' and cell volume of BIT, BLT and BLTM for some planes

Sample	Planes	Lattice constant			Cell volume (nm^3)
		a (nm)	b (nm)	c (nm)	
BIT	(200), (028), (008)	0.54	0.54	3.27	0.96
BLT	(200), (028), (008)	0.54	0.54	3.29	0.96
BLTM	(200), (028), (008)	0.54	0.54	3.28	0.96

3.2 Study of IR Spectroscopy

To collect IR spectra of a sample various techniques can be employed for placing the sample in the path of infrared beam depending upon whether the sample is gas or solid or liquid. For solid materials alkali halide, KBr pellet technique is well established. In this work solid samples were grounded in a clean mortar to a fine powder and weighted quantity of the powder was mixed intimately with desiccated highly purified (99.99%) alkali halide, KBr powder. The mixture was then pressed in a pressure gauge to yield a pellet of approximate thickness 0.11mm suitable for mounting in the spectrometer. All infrared spectra of the samples were collected by FTIR spectrophotometer (spectrum 100, Perkin Elmer) situated at the Central Science Laboratory, University of Rajshahi over the range of wave number 2000 – 300 cm^{-1} . The resolution of the instrument was 1 cm^{-1} .

Fig. 6 shows the IR spectra of pure $\text{Bi}_4\text{Ti}_3\text{O}_{12}$ (BIT) powder calcined at 800 °C for 4 hours. From the Fig. 6, it is found that two sharp absorption peaks appear at 814 and 592 cm^{-1} which corresponds to the stretching vibrations of Bi-O and Ti-O bonds respectively. Another sharp absorption peak appears at 379 cm^{-1} that is related to the bending vibrations of Ti-O bonds [5]. In addition, two shoulder peaks are observed at 470 and 313 cm^{-1} . The appearance of absorption peaks at 814, 592 and 379 cm^{-1} is a characteristics feature of the formation of titanate structure.

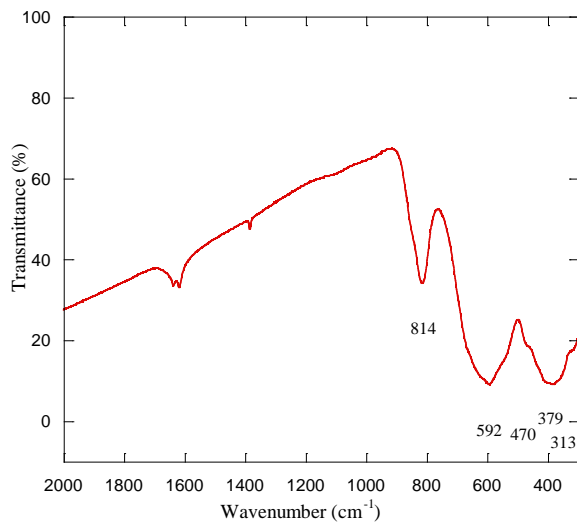


Fig.6: FTIR spectra of $\text{Bi}_4\text{Ti}_3\text{O}_{12}$ (BIT) powder calcined at 800 °C for 4 hours

The IR spectra of La doped BIT, $\text{Bi}_{3.25}\text{La}_{0.75}\text{Ti}_3\text{O}_{12}$ (BLT) is shown in Fig. 7. From the Fig. 7, it is found that the IR spectra of BLT powder were similar to those of BIT powder, except small shifts of the absorption peaks with reduction of the intensities. The adsorption peaks at 592 cm^{-1} and 379 cm^{-1} were shifted to higher wave numbers of 607 cm^{-1} and 392 cm^{-1} respectively in the IR spectra of BLT, while the intensity of the band at 814 cm^{-1} is significantly decreased [5]. It is also found that the shoulder peaks observed at 470 and 313 cm^{-1} in BIT disappeared due to La doping (at 0.75). It is well known that crystal structure of pure BIT is monoclinic [3]. The monoclinic phase undergoes a structural phase transition to orthorhombic due to La doping at 0.66 doping level [3]. Therefore, the disappearance of shoulder peaks at 470 and 313 cm^{-1} could be related to the monoclinic to orthorhombic phase transition, which is consistency with XRD result.

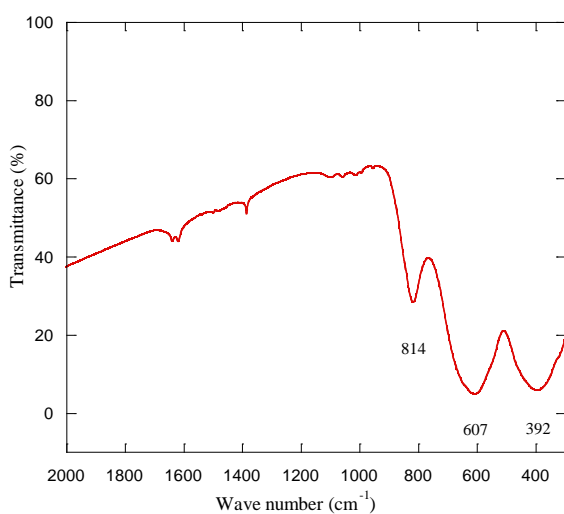


Fig.7: FTIR spectra of $\text{Bi}_{3.25}\text{La}_{0.75}\text{Ti}_3\text{O}_{12}$ (BLT) powder calcined at 800 °C for 4 hours

The comparison of the IR spectra of BIT and BLT powder is shown in Fig. 8.

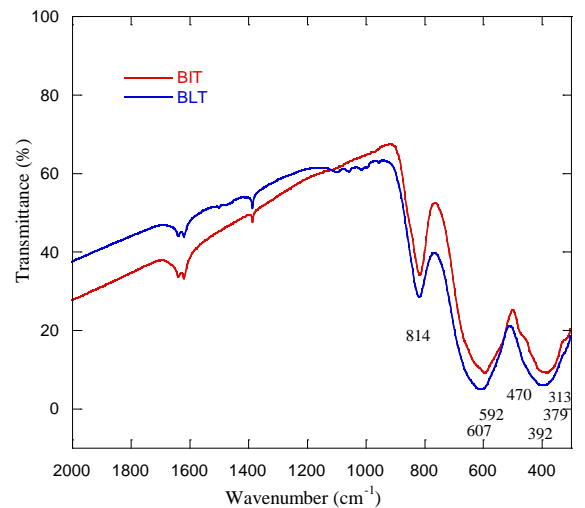


Fig.8: FTIR spectra of BIT and BLT powder calcined at 800 °C for 4 hours

Fig. 9 shows the combined FTIR spectra of La and Mn co-doped BIT, $\text{Bi}_{3.25}\text{La}_{0.75}\text{Ti}_{3-x}\text{Mn}_x\text{O}_{12}$ ($x = 0.005, 0.01, 0.02$). It is obvious that as the doping level of Mn in BLT increase, there is a dramatic change of the IR spectra is observed. The absorption peaks at 607 cm^{-1} and 392 cm^{-1} become defused as shown in the Fig. 9. Moreover, a new and relatively broad absorption peak appeared around 1015 cm^{-1} , which may related to the stretching vibration of Mn-O bonds. Therefore, it is reasonable to speculate that the new absorption peak resulting from the Mn-O vibrational mode could be due to the replacement of Ti by Mn in the TiO_6 octahedron. The intensity of this peak gradually increases with the increase of Mn doping level. The gradual enhancement of the new absorption peak with the increase of Mn-doping level further confirms the Mn substitution at the B site in BLTM ceramic samples.

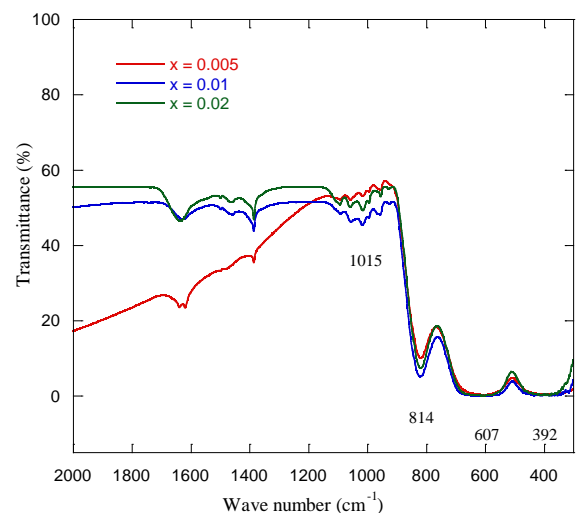


Fig.9: FTIR spectra of La and Mn co-doped BIT, $\text{Bi}_{3.25}\text{La}_{0.75}\text{Ti}_{3-x}\text{Mn}_x\text{O}_{12}$ ($x = 0.005, 0.01, 0.02$) powder calcined at 800 °C for 4 hours

A combined FTIR spectra of BIT, BLT and BLTM ($x = 0.005, 0.01$ & 0.02) samples is shown in Fig. 10.

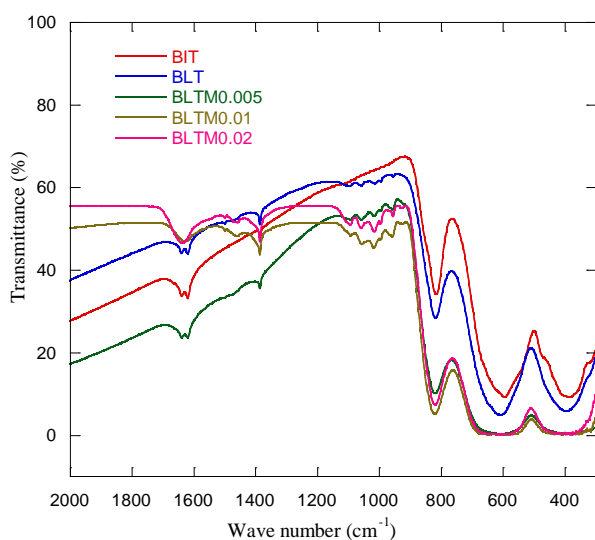


Fig.10: Combined FTIR spectra of BIT, BLT and BLTM ($x = 0.005, 0.01, 0.02$) powder calcined at 800 °C for 4 hours

3.3 Dielectric Properties

The dielectric constant vs Mn doping concentration of $\text{Bi}_{3.25}\text{La}_{0.75}\text{Ti}_{3-x}\text{Mn}_x\text{O}_{12}$ ($x = 0, 0.005, 0.01$ and 0.02) samples at different frequencies is shown in the Fig. 11. From the Fig. 11, it is clear that the dielectric constant increases first with the increase of Mn content and it reaches the highest value at $x = 0.01$ then the dielectric constant decrease with the increase Mn content. The optimum Mn doping level in BLT towards the better dielectric performance is 0.01.

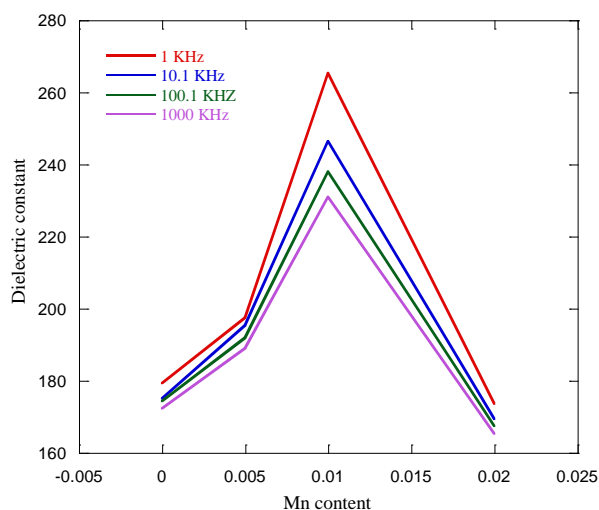


Fig.11: Variation of dielectric constant with Mn doping concentration of $\text{Bi}_{3.25}\text{La}_{0.75}\text{Ti}_{3-x}\text{Mn}_x\text{O}_{12}$ ($x = 0, 0.005, 0.01$ and 0.02) samples at different frequencies

4. CONCLUSIONS

BIT, La doped BIT and La and Mn doped BIT ceramic samples had been prepared by solid-state reaction method. The influence of La and Mn doping in BIT were investigated. From XRD and IR result it can be concluded that the pure and doped BIT ceramic samples successfully fabricated. A structural monoclinic to

orthorhombic phase transition observed due to the La (0.75) doping. The dielectric constant increases as La is doped in pure BIT. The dielectric constant further increases with Mn doping at a certain limit and then decrease due to the domain wall pinning. From the results it is observed that BLTM sample shows the best result for the Mn doping level at 0.01.

5. ACKNOWLEDGEMENT

The authors are grateful to the Materials science division, Atomic Energy Commission, Dhaka, Bangladesh for providing laboratory facilities. The authors give thanks to the Ministry of Science and Information & Communication Technology (MOSICT) of Peoples Republic of Bangladesh for financial support.

6. REFERENCES

- [1] M. Raghavvender, G. S. Kumar and G. Prasad, "Electrical properties of La-modified strontium bismuth titanate", *Indian Journal of Pure & Applied Physics*, Vol. 44, pp. 46-51, 2006.
- [2] I. A. Zarubin, V. G. Vlasenko, A. T. Shuvaev, G. P. Petin, and E. T. Shuvaeva, "Effect of Doping on the Crystal Structure and Dielectric Properties of the Aurivillius Phase $\text{CaBi}_4\text{Ti}_4\text{O}_{15}$ ", *Bulletin of the Russian Academy of Sciences: Physics*, Vol. 72, No. 10, pp. 1406-1409, 2008.
- [3] B. D. Stojanovic, C. O. Paiva-Santos, M. Cilense, C. Jovalekic, Z. Z. Lazarevic, "Structure study of $\text{Bi}_4\text{Ti}_3\text{O}_{12}$ produced via mechanochemically assisted synthesis", *Materials Research Bulletin*, Vol. 43, pp. 1743-1753, 2008.
- [4] X. L. Zhong, J. B. Wang, L. Z. Sun, C. B. Tan, X. J. Zheng and Y. C. Zhou, "Improved ferroelectric properties of bismuth titanate films by Nd and Mn cosubstitution", *Applied Physics Letters*, vol. 90, No. 012906, pp. 1-3, 2007.
- [5] Y. Kan, X. Jin, G. Zhang, P. Wang, Y. B. Cheng and D. Yan, "Lanthanum modified bismuth titanate prepared by a hydrolysis method", *Journal of Materials Chemistry*, Vol. 14, pp. 3566-3570, 2004.
- [6] W. F. Yaoa, H. Wang, X. H. Xua, J. T. Zhoua, X. N. Yang, Y. Zhang and S. X. Shang, "Photocatalytic property of bismuth titanate $\text{Bi}_2\text{Ti}_2\text{O}_7$ ", *Applied Catalysis A: General*, Vol. 259, No. 1, pp. 29-33, 2004.
- [7] W. Li, A. Chen, X. Lu and J. Zhu, "Collective domain-wall pinning of oxygen vacancies in bismuth titanate ceramics", *Journal of Applied Physics*, Vol. 98, 2005.
- [8] J. S. Kim, S. Y. Lee, H. J. Lee, C. W. Ahn, I. W. Kim, and M. S. Jang, "Control of the ferroelectric and electrical properties of Nd substituted bismuth titanate ceramics", *Journal of Electroceramics*, Vol. 21, pp. 633-636, 2008.

7. NOMENCLATURE

Symbol	Meaning	Unit
T	Temperature	(K)
θ	Angle	(degree)